

Experimental Analysis of Control in Electric Vehicle Charging Station Based Grid Tied Photovoltaic-Battery System

A. Hassoune, M. Khafallah, A. Mesbahi, T. Bouragba

Abstract—This work presents an improved strategy of control for charging a lithium-ion battery in an electric vehicle charging station using two charger topologies i.e. single ended primary inductor converter (SEPIC) and forward converter. In terms of rapidity and accuracy, the power system consists of a topology/control diagram that would overcome the performance constraints, for instance the power instability, the battery overloading and how the energy conversion blocks would react efficiently to any kind of perturbations. Simulation results show the effectiveness of the proposed topologies operated with a power management algorithm based on voltage/peak current mode controls. In order to provide credible findings, a low power prototype is developed to test the control strategy via experimental evaluations of the converter topology and its controls.

Keywords—Battery charger, forward converter, lithium-ion, management algorithm, SEPIC.

I. INTRODUCTION

IN recent years, the increased emission of greenhouse gases and the decreased level of fossil fuels reserve have caused a shortage of energy sources in power systems based petroleum products [1]. Furthermore, the adoption of distributed power generation has received high attention owing to its various benefits, as the improved accuracy, stability and decreasing the energy losses within the conversion energy devices (CED). Another advantage of the CED is presented during the process of establishing a hybrid energy source, which has different platforms and methods of control.

The integration of renewable energy sources in the power systems based grid in a standalone mode has become the topic of several researches [2]. The intermittent in solar irradiance and in wind speed are both the starting point where an accurate CED would set the required control to obtain quite a high level of efficiency [3]. A suitable power converter is used in multiple frameworks e.g. extracting the maximum power from PV cells and from variable speed of wind turbine blades. Apart the control method, the architecture of the CEDs is often

considered important to be fitted with extra features for instance, high power yield and stability of voltage/current rates in both sides, input and output of electrical devices [4].

The electric vehicle charging station (EVCS) is presented as one of the main applications of the chargers, the station uses almost all the CEDs i.e., DC/DC, DC/AC, AC/DC and AC/AC. Recently, various topologies of EVCS are discussed in the literature in order to achieve optimization goals [5]. A typical diagram is based on a DC link medium voltage, connects all renewable energy sources via specific converters with all kinds of loads for instance, EV batteries and residential AC loads; however, the grid would be eventually an addition to the platform [6].

The number one priority of a CS customer is to charge his vehicle battery through a rapid charging process. In the meanwhile, the EVCS infrastructure must be equipped with the suitable technologies of converters in order to fulfill the required rate of charging power from each plugged in EV [7]. According to [8], superchargers of 350 kW are designed to feed the EV battery within eight minutes, to support this great amount of energy flow in a short time, the battery technology must handle the high injected current to preserve the battery performance from overheating phenomenon and other inconvenient constraints [9]. Thus, the power supply system of the EVCS is now under a massive power demand, especially when several vehicles are connected at the same time. The converters as well must be designed by which their components could bear the burden from the imposed power/frequency [10].

This work provides a comparison study between two different topologies of DC/DC converters i.e., forward converter and single ended primary inductor converter (SEPIC) operated in both modes i.e., buck and boost. The accuracy, the stability and the rapidity of control would be tested under fast variations of the input current ripples [11]. Furthermore, an electrical system charger is often being a critical component in which an isolated converter is required to get separate grounds due to the high frequency transformer providing this feasibility. The isolated converter is featured by its outlet that can be set to be either positive or negative. Additionally, the forward converter along with flyback converter are known as low power isolated CEDs, they are both representing an improved version of the classic DC/DC converters where many enhancements are implemented e.g., increased noise immunity [12]. In this project, a 50W low power prototype of a charger and lithium-ion battery, are set to

A. Hassoune is with the Laboratory of Energy & Electrical Systems (LESE), Superior National School of Electricity and Mechanical (ENSEM), Hassan II University of Casablanca-20470, Casablanca-Morocco (phone: +212-672-524-441; e-mail: a.hassoune@IEEE.org).

M. Khafallah and A. Mesbahi are with the Laboratory of Energy & Electrical Systems (LESE), Superior National School of Electricity and Mechanical (ENSEM), Hassan II University of Casablanca-20470, Casablanca-Morocco.

T. Bouragba is with the Engineering School of Industrial Systems (EIGSI Casablanca)- 282 Route de l'Oasis, 20103 Casablanca -Morocco.

simulate each converter topology under voltage mode control (VMC) and peak current mode control (CMC). Meanwhile, a power management algorithm is used in this work to set up the two controls in order to integrate all these criteria in one efficient platform [13].

The paper is divided as follows. Section I introduces the used approach. The control strategy and the description of the adopted DC/DC converters are presented in Section II. Design and simulation results in MATLAB/Simulink of the forward converter and the SEPIC operated under VMC and peak CMC are performed in Section III. Experimental results of the architecture are analyzed in Section IV. Conclusions of this paper are provided in Section V.

II. ARCHITECTURE OF THE PROPOSED CONVERTER TOPOLOGIES

A. Forward Converter

Derived from the traditional diagrams of DC/DC converters, the forward converter based single transistor composed by a transformer and that refers to galvanic isolation, is an accurate choice for specific applications [14]. Technically, using a transformer based converter to boost the voltage is an option where the turns ratio would improve the converter response in terms of providing a high voltage gap between input and output. Fig. 1 shows the schematic of the single transistor forward converter charging a lithium-ion battery.

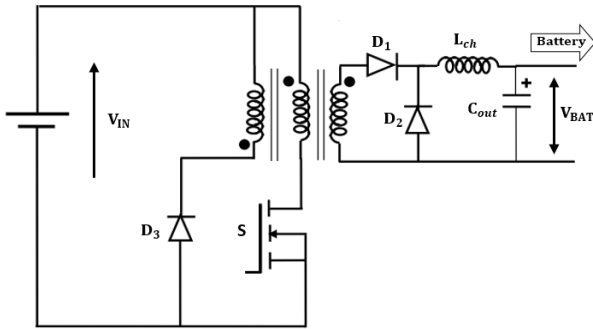


Fig. 1 Schematic of a single transistor forward converter

Unlike a classical buck/boost converter, this scheme contains a transformer instead of inductors which reduces the air gap due to the high magnetizing inductance of the transformer [15]. Yet, the energy transfer during the conduction phase of the transistor is not stored. The output voltage of the forward converter is expressed in (1).

$$V_{BAT} = V_{IN} \frac{N_s}{N_p} D_C \quad (1)$$

where, V_{IN} is the input voltage, V_{BAT} is the battery voltage, N_p and N_s are the number of winding turns of a transformer, primary and secondary, respectively, and D_C is the duty cycle of the transistor generated by a pulse width modulation.

The basic operation of the forward converter can be

summarized as: Once the control drive is set to the transistor (S), the energy would drop through D_1 , L_{ch} , and into the battery. At this time, the magnetizing current starts to accumulate in the transformer primary. When the transistor is closed, then the magnetizing current would be dissipated into the primary windings. The magnetizing current keeps to flow through the demagnetizing winding and D_3 , meanwhile, D_2 is allowing the dissipation of the output current from L_{ch} to the load, while the magnetizing current goes down to zero via D_3 [16].

B. Single Ended Primary Inductor Converter (SEPIC)

The SEPIC is one of the conventional topologies and many industrial applications are based on its features, such as power factor correction, LED driving, and applications where a symmetric output voltage is required. Basically, all the topologies of power converters with input inductor are used to decrease the input current ripple. The inductor offers a trade-off between the input current ripple and the DC/DC converter dynamic response. Compared to the buck/boost converter, SEPIC has the same voltage polarity as the input that is its main advantage [17]. Fig. 2 shows the scheme of SEPIC. When the power switch is turned on, the voltage set-up and when the switch is turned off the voltage drops. During the steady-state process, the ripple voltage would be neglected.

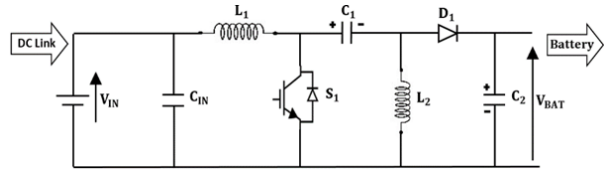


Fig. 2 Schematic of SEPIC

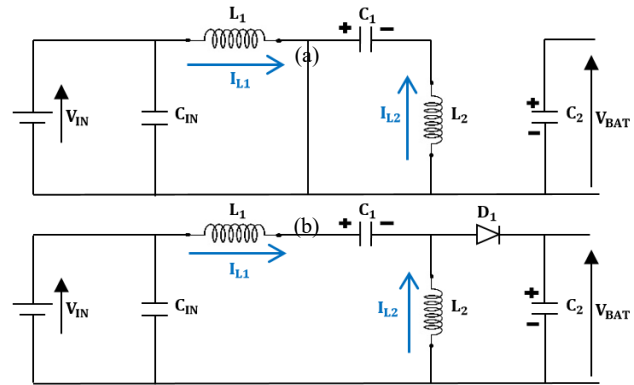


Fig. 3 SEPIC during CCM operation when S_1 is (a) on, and (b) off

In order to explain the operating phases of SEPIC, it is important to analyze the scheme taking into account the two conduction states of the transistor (S_1) during continuous conduction mode (CCM) i.e., opened in the first phase and closed in the second. Besides, a CCM is a state when the inductor current (V_{L1}) never goes down to zero. During the steady-state operation, the average voltage across capacitor C_1 is equal to the input voltage (V_{IN}). Fig. 3 illustrates the SEPIC

operating in CCM, the voltage across D_1 is neglected [18].

At first, the transistor closes, L_1 connected to the V_{IN} , the current through L_1 increased with a constant slope. Once the transistor opens, L_1 current would charge C_1 . The voltage value of L_1 and L_2 during the switch S_1 on-time can be detailed as:

$$V_{L1} = V_{IN} \quad (2)$$

$$V_{L2} = V_{C1} \quad (3)$$

During the S_1 off-time, the input inductor voltage (V_{L1}) and the voltage across L_2 can be expressed as:

$$V_{L1} = V_{IN} - V_{C1} - V_{BAT} \quad (4)$$

$$V_{L2} = -V_{BAT} \quad (5)$$

In steady state, the inductors voltage is zero, which leads to a constant current. Thus the volt-second formula of L_1 and L_2 are described as:

$$V_{IN} D_S T_S + (V_{IN} - V_{C1} - V_{BAT})(1 - D_S) T_S = 0 \quad (6)$$

$$V_{C1} D_S T_S - V_{BAT}(1 - D_S) T_S = 0 \quad (7)$$

where, D_S is the duty cycle of S_1 expressed in (8).

$$D_S = \frac{t_1 - t_0}{T_S} \quad (8)$$

From (6) and (7) the ratio between V_{BAT} and V_{IN} can be determined as:

$$V_{BAT} = V_{IN} \frac{D_S}{1 - D_S} \quad (9)$$

As per specifications, the inductor ripples current (ΔI_L) is a critical standard in order to design a reliable SEPIC. A rule of thumb is to set 20% to 40% of the input current (I_{IN}), as calculated in (10). Additionally, too much ripples might cause a high rate of electromagnetic interference while too little would make the PWM generator unstable [19].

$$\Delta I_L = 30\% \frac{I_{IN}}{\eta} \quad (10)$$

In order to adapt an accurate estimation of the input current, I_{IN} is divided by the worst efficiency rate (η) at $V_{IN} = V_{IN(min)}$ and $I_{OUT} = I_{OUT(max)}$. To achieve a fast and a stable reaction for charging the battery within safety measurements, the control would be based on PI method [20].

C. Voltage and Peak CMC

In accordance with the adopted application and to provide continuous control of a power system, the VMC and the peak CMC are regulating each operating mode, with only one control at a time. They are designed to obtain numerous improvements, for instance, a fast reaction to any required charging power rate [21]. The selected process of control is started with programming the voltage mode and peak current mode set points, which are available to the user. Besides, the maximum output voltage and the supply current can be controlled at any operating mode. Fig. 4 depicts both the CMC and the VMC.

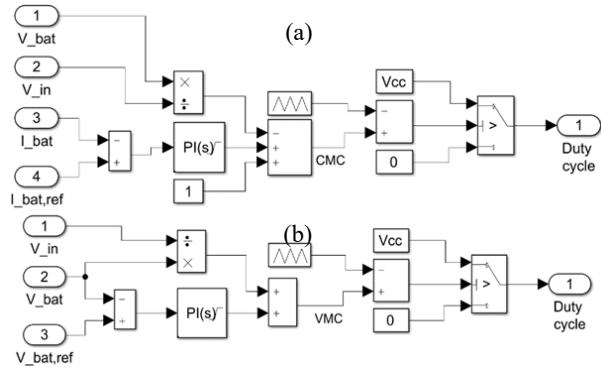


Fig. 4 Operating mode control (a) current (b) voltage

Since the power supply system operates at peak current mode, its input provides a constant current injected into a large scale of load voltage even at short circuit circumstances.

D. Battery Model

The most relevant features of a battery are its specific energy and power, safety and durability. The lithium-ion battery is one of the effective storage technologies, it has highly performant features i.e., operating under wider temperature range, it supports higher injected current within a short time and a less self-discharge [22]. Fig. 5 shows the three operating phases of charging a lithium ion battery.

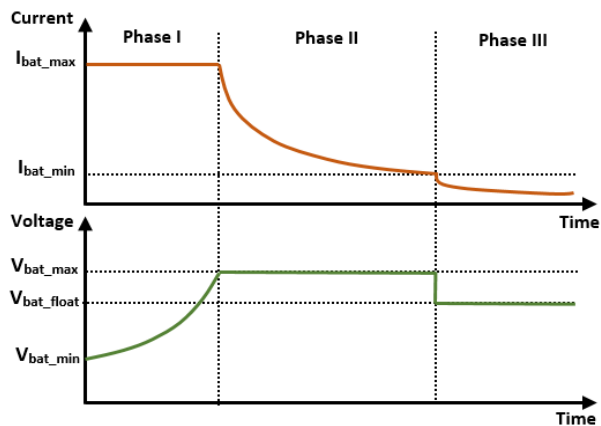


Fig. 5 Battery charging phases

As can be seen from Fig. 5, the battery charger is typically operated under three stages: first one is controlled with CMC in which the reference current is set to $I_{bat-max}$ in order to avoid the battery overheating [23].

Once V_{bat} across $V_{bat-max}$, the battery charging mode would be switched to the second stage and the approach would be adjusted to the VMC in which the output voltage is configured to $V_{bat-max}$. Meanwhile, I_{bat} is reduced until it falls under $I_{bat-min}$ where the third stage is achieved; the control strategy is still operating at the same mode, except that the reference voltage is now set to $V_{bat-float}$. This rate is able to avoid the worst deep self-discharge by generating a small current for charging the battery.

III. SIMULATION RESULTS

In order to test the effectiveness of these topologies and their control strategies, a design of a 50W battery charger is modeled in MATLAB/Simulink. The finding is to set a comparative approach between SEPIC and forward converter, where the load is as a 12V/2Ah lithium-ion battery. Fig. 6

illustrates the two schemes of the adopted CEDs modeled in the Simulink tool. The power management algorithm is used to control both converters by which a generated duty cycle is based on PI control and on dynamic inputs of voltage/current.

The proposed control is chosen via numerous criteria, e.g., the real time monitoring of the charging process in order to get a reliable data to validate the configured control mode and for a display purpose [24]. The specification of the proposed converters used in simulation is given in Table I.

TABLE I
50W BATTERY CHARGER SETTINGS

	Forward converter	SEPIC
Input voltage (V_{IN})	20 V	20 V
Battery Voltage/Capacity (V_{BAT}/C_{BAT})	12 V/ 2 Ah	12 V/ 2 Ah
Frequency (F_{EQ})	70 kHz	70 kHz
Inductor (L)	$L_1 = 10$ mH $L_2 = 12$ mH	$L_{CH} = 5$ mH
Capacitor (C)	$C_1 = 80$ uF $C_2 = 50$ uF	$C_{OUT} = 20$ uF

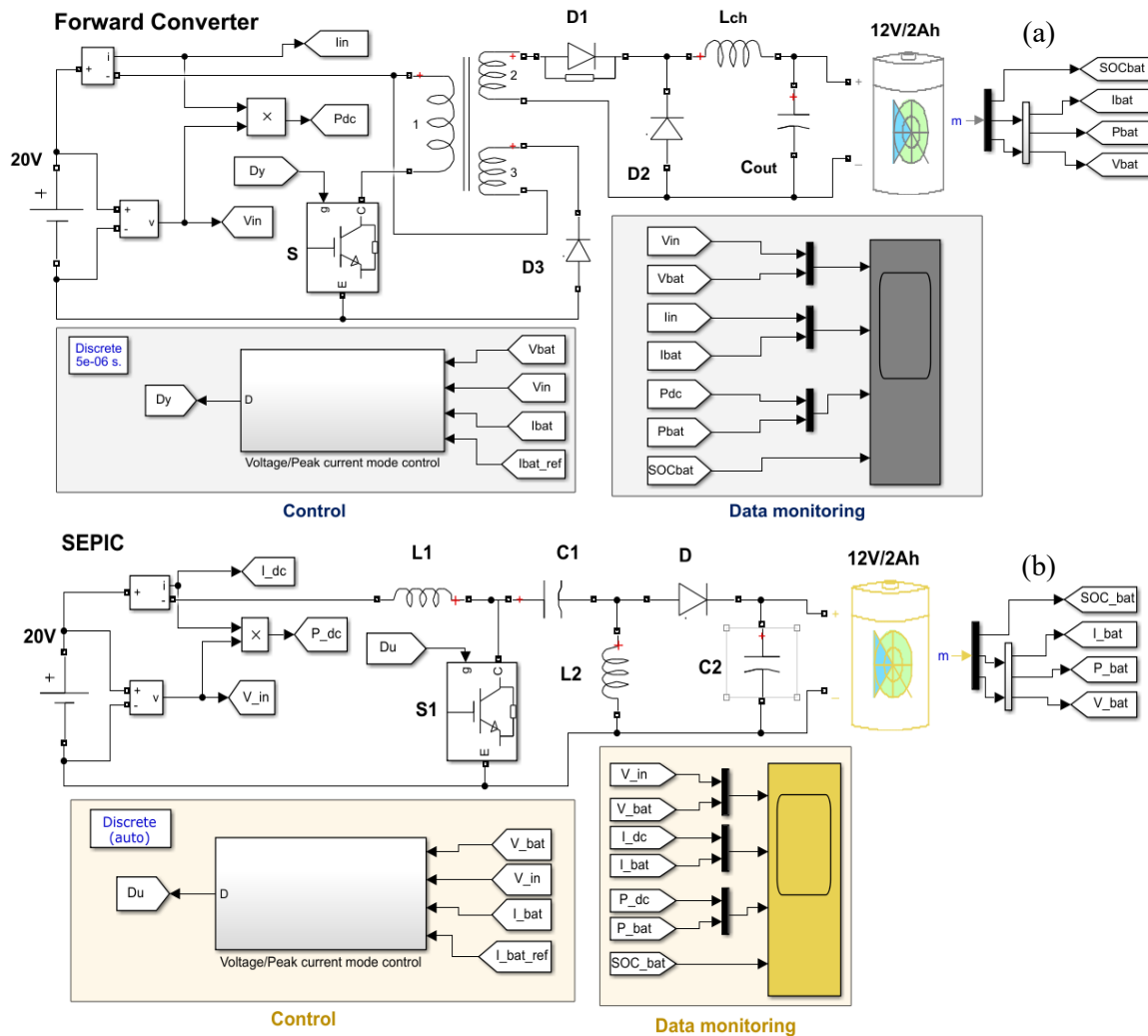


Fig. 6 Designed converters in Simulink a) Forward b) SEPIC

The simulation features are based, on the one hand, on a comparative study between two topologies of DC/DC converter, on the other hand, on a mixed control strategy and its effectiveness on the charging operation of the lithium-ion battery. The goal is to gain as much as possible from each control mode by which the battery electrical characteristics would be preserved from eventual performance degradation. Thus, the overheating situation is often caused by a charging/discharging overcurrent. In accordance with the project specification, the operation is started with the peak CMC to avoid an uncontrolled first charging stage, once the battery voltage reaches 12V, the power management unit will switch the control into the VMC in order to achieve more revenues from a large scale of power offered by the 50W charger. Fig. 7 illustrates the simulation results of a battery

charger based forward converter operated under peak current control. This case scenario is used in numerous applications, for instance, charging storage batteries in the EVCS.

A constant current control is set by which the lithium-ion battery can be charged by a maximum power, thus the SOC waveform is presenting one slope rate. As it can be seen, the charging battery voltage crosses its maximum limit at $t=4.6$ min, this overvoltage will be increased in an uncontrolled process which will cause harmful sides effects to the battery [25].

To take safety measurement of the selected charging operation, the power management unit is added to the platform in order to adapt the two modes of control following the main algorithm. Fig. 8 shows the proposed approach designed in Simulink using MATLAB function block [26].

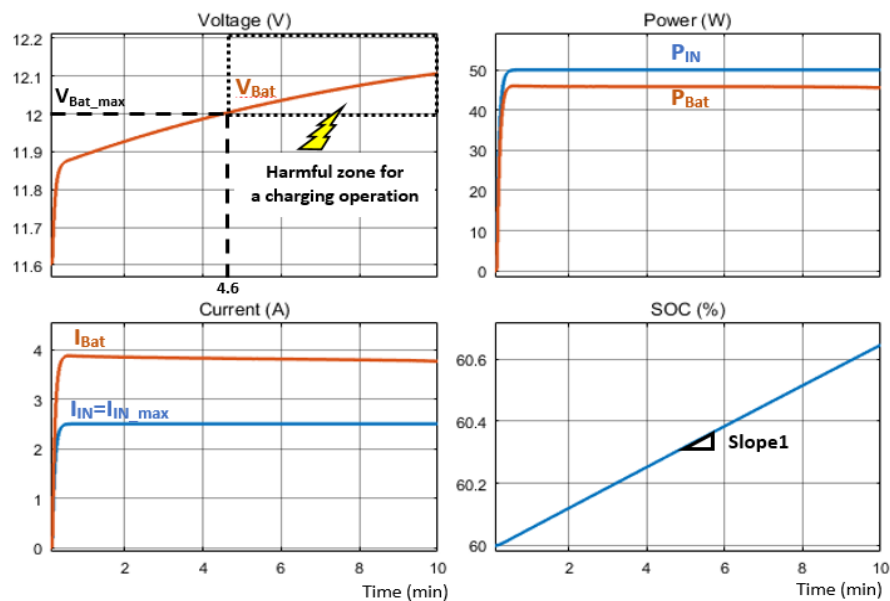


Fig. 7 Waveforms of the CMC applied on forward converter vs. time

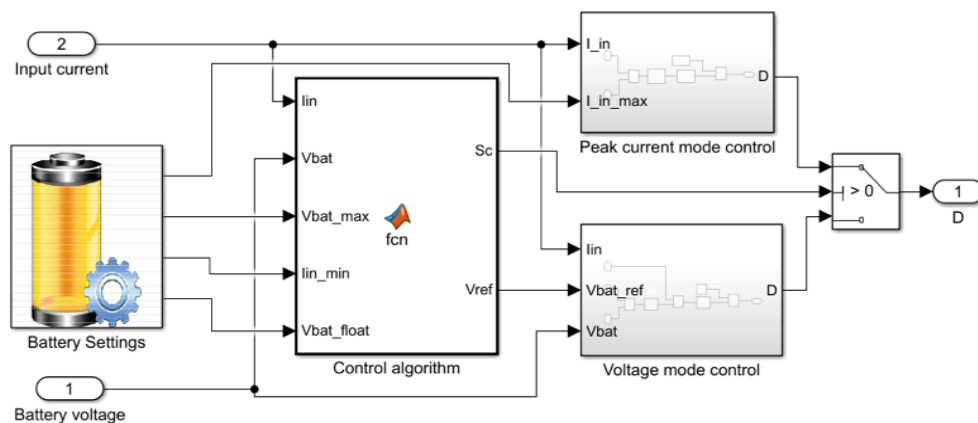


Fig. 8 Control management algorithm of the system

The program starts the operation by sensing all the dynamic data i.e., voltage/current of the battery and the supply input

current. In the meanwhile, the lithium-ion battery is charging within its allowed limits of the injected current and the output

charging voltage. Fig. 9 illustrates the results of the improved charging process using the previous algorithm.

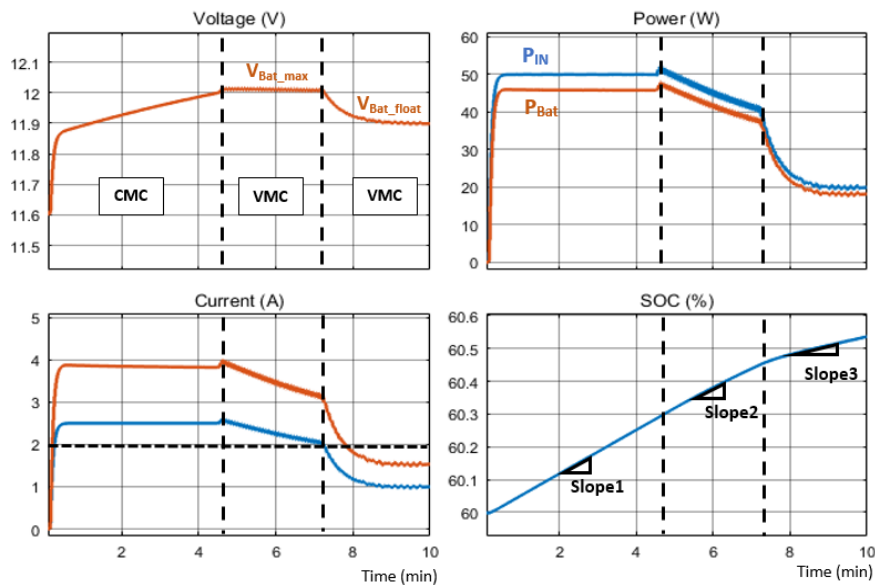


Fig. 9 Waveforms of the hybrid control applied on forward converter vs. time

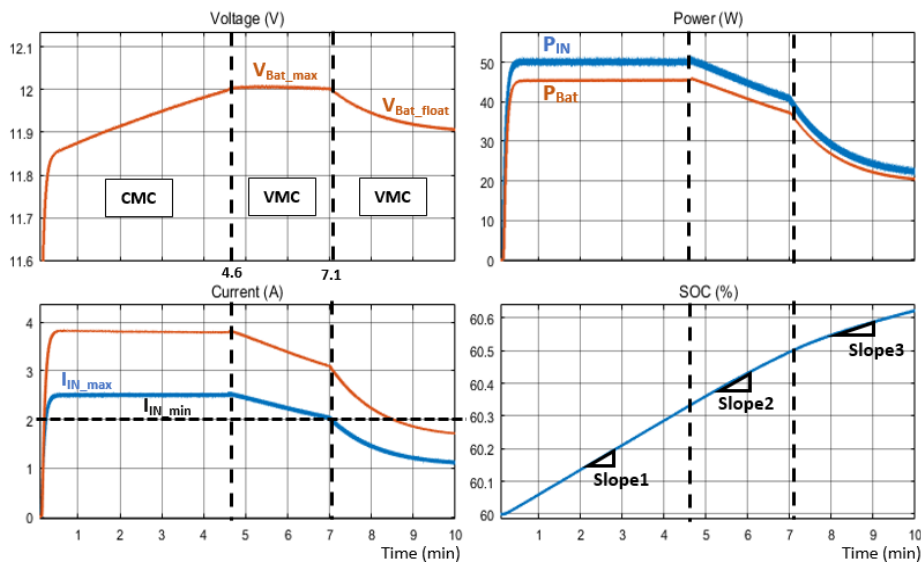


Fig. 10 Waveforms of the hybrid control applied on SEPIC versus time

From $t=0-4.6$ min, the charger is operated under CMC where I_{IN} is fixed to I_{IN-max} , after $t=4.6$ min, the battery voltage reached $V_{Bat-max}$. In order to stabilize the charging voltage rate, the control algorithm is switched to the VMC, where the reference voltage would maintain the output to $V_{Bat-max}$. At $t=7.1$ min, the injected current goes down below I_{IN-min} , the VMC would be adjusted to the second reference voltage ($V_{Bat-float}$).

The next chapter of the simulation section is to validate the algorithm on another topology of converters as the case of SEPIC. Fig. 10 shows the results of a SEPIC running under

both the peak current and the VMC. The SOC of the 12V battery identifies three rates of slope due to the changes in charging power throughout the simulation time.

The waveforms of Fig. 10 test the theoretical approaches of charging a battery using various modes of control performed at the same process. As results, all fixed goals are achieved as preserving the battery from an eventual overheating caused by overvoltage and overcurrent, and also the profitability in terms of a flexible control. Yet, the charging power in the second stage of SEPIC is less stable than the forward operating mode.

IV. EXPERIMENTAL EVALUATION

A laboratory prototype of the used architecture is implemented in order to test the proposed control strategies. The charging operation is controlled by Texas instrument Solar Explorer Kit (TMDSSOLAR PEXPKIT). It offers a flexible and efficient low voltage platform to assess the C2000 microcontroller family for power applications. Fig. 11 shows the printed circuit board (PCB) of the solar kit, in which the proposed control strategies would be verified. The PCB is shipped with F28035 control card to drive the SEPIC, DC/DC boost converter and the inverter. However, the PV array is emulated via a synchronous buck boost stage controlled by Piccolo-A F28027 card.

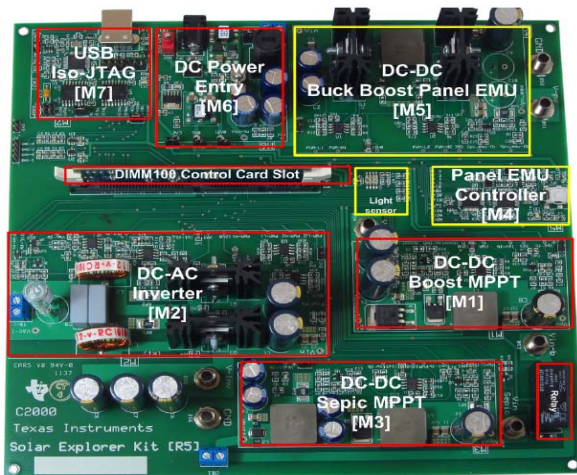


Fig. 11 Macro Blocks of Solar Explorer Kit

The prototype contains several stages for DC to DC and DC to AC conversion along with a detection communication to

operate the MPP Tracking. A PV emulator is built onto the board with a DC/DC power stage using light sensor. To complete the demonstration, a lithium-ion battery is integrated to perform the 12V/2Ah battery. However, Fig. 12 illustrates the test bench setup of the proposed approach.

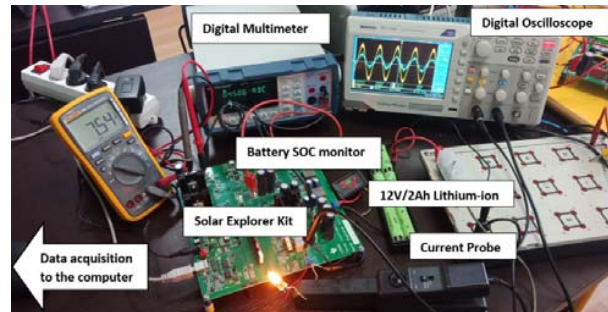


Fig. 12 Experimental prototype of battery charging process

During the operation modes, further precautions are set in order to get the system matches the required project specification. Table II shows the allowed margin of the connected load electrical characteristics.

TABLE II
POWER STAGE PARAMETERS OF THE SEPIC

Voltage (V)		Current (A)		Power rating	Frequency
Input	Output	Input	Output	max (W)	(kHz)
0-30	10 - 16	0-3.5	0-3.5	50	200

In this mode, a typical 12 V/2 Ah is adopted to test the 50W PV emulator, the battery charger would be operated under a hybrid strategy of control. The charger frequency uses 200 kHz which will reduce the input inductor ripples. Furthermore, Figs. 13 and 14 show the voltage, current and the power at the input and at the output of SEPIC, respectively.

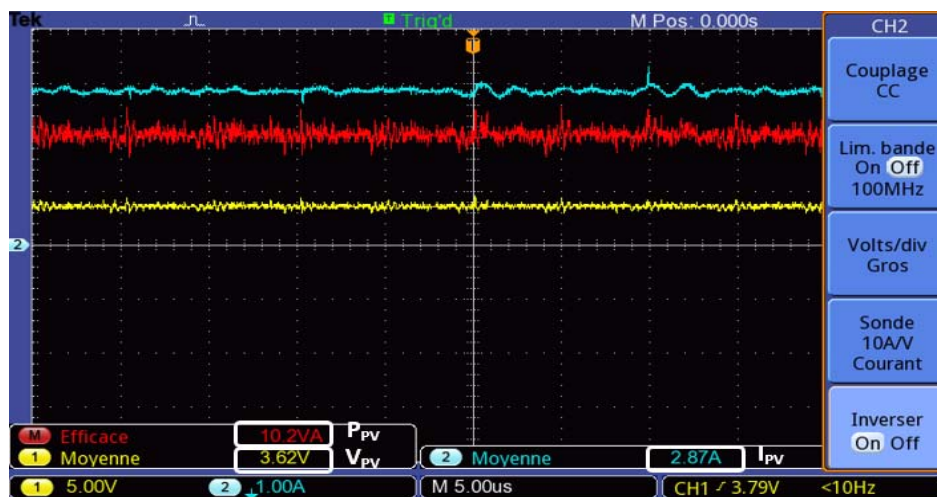


Fig. 13 Experimental results of DC voltage, current and power at SEPIC Input vs. time

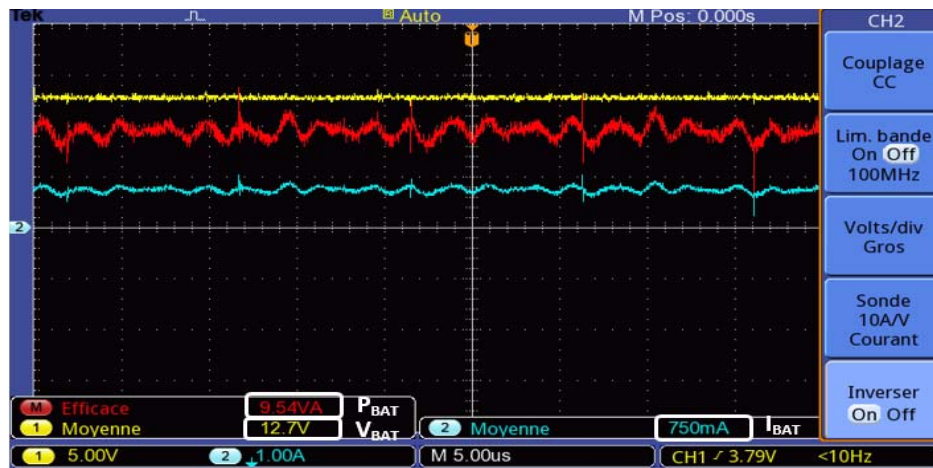


Fig. 14 Experimental results of DC voltage, current and power at SEPIC Output vs. time

As follows from the results of Fig. 14, the SEPIC is operated at boost mode due to the low irradiance rate applied in the PV emulator input (0.2 kW/m^2), at this case, the PV provides 3.62V . However, the electrical efficiency of the system reaches 93.5% . From the adopted battery datasheet, an overcharge voltage is set to $V_{OC}=15\text{V}$, the condition in which the controller would switch the control to VCM is when the battery voltage exceeds $0.95 V_{OC}$ (14.25V), such case is depicted in Fig. 14, where V_{BAT} still at $0.86 V_{OC}$ (12.7V).

Recent advanced technologies of batteries are designed in order to support higher injected current and to operate under a large scale of charging voltage. Thus, with the proposed control strategies, the charging operation would achieve beneficial findings, depend on the battery capacity and on its features.

V.CONCLUSION

In this paper, a control algorithm is presented in detail to charge a lithium-ion battery with quite a high level of accuracy and stability. From the proposed schemes of converters, the control strategies via peak CMC and VMC achieved productive results while considering numerous criteria, for instance the battery capacity, the rated power of the adopted charger and how the management algorithm would react rapidly to the frequent changes in charging voltage/current. The simulation results performed in Simulink tool had validated the proposed control techniques on two different topologies of converters i.e., forward converter and SEPIC. The findings are analyzed with experimental evaluations using a low power solar kit, by which multiple approaches were tested on the charging/discharging process of a lithium-ion battery.

REFERENCES

- [1] A. Moro and L. Lonza, "Electricity carbon intensity in European Member States: Impacts on GHG emissions of electric vehicles," *Transportation Research Part D: Transport and Environment*, vol. 64, pp. 5–14, Oct. 2018.
- [2] K. Engeland, M. Borga, J.-D. Creutin, B. François, M.-H. Ramos, and J.-P. Vidal, "Space-time variability of climate variables and intermittent

renewable electricity production – A review," *Renewable and Sustainable Energy Reviews*, vol. 79, pp. 600–617, Nov. 2017.

- [3] A. Luo, Q. Xu, F. Ma, and Y. Chen, "Overview of power quality analysis and control technology for the smart grid," *Journal of Modern Power Systems and Clean Energy*, vol. 4, pp. 1–9, Jan. 2016.
- [4] N. Tewari and V. T. Sreedevi, "A novel single switch dc-dc converter with high voltage gain capability for solar PV based power generation systems," *Solar Energy*, vol. 171, pp. 466–477, Sep. 2018.
- [5] A. Hassoune, M. Khafallah, A. Mesbahi, and D. Breuil, "Electrical design of a photovoltaic-grid system for electric vehicles charging station," *2017 14th International Multi-Conference on Systems, Signals & Devices (SSD)*, Mar. 2017.
- [6] S. Chalise, J. Sternhagen, T. M. Hansen, and R. Tonkoski, "Energy management of remote microgrids considering battery lifetime," *The Electricity Journal*, vol. 29, no. 6, pp. 1–10, Jul. 2016.
- [7] S. Rivera and B. Wu, "Electric Vehicle Charging Station With an Energy Storage Stage for Split-DC Bus Voltage Balancing," *IEEE Transactions on Power Electronics*, vol. 32, no. 3, pp. 2376–2386, Mar. 2017.
- [8] "ABB Launching 350 kW EV Fast Charger At Hannover Messe (Online). Available: <https://cleantechnica.com/2018/04/25/abb-launching-350-kw-ev-fast-charger-at-hannover-messe/> (Accessed: 25-April-2018).
- [9] L. Pan and C. Zhang, "Performance Enhancement of Battery Charger for Electric Vehicles Using Resonant Controllers," *Energy Procedia*, vol. 105, pp. 3990–3996, May 2017.
- [10] F. Roccaforte, P. Fiorenza, G. Greco, R. Lo Nigro, F. Giannazzo, F. Iucolano, and M. Saggio, "Emerging trends in wide band gap semiconductors (SiC and GaN) technology for power devices," *Microelectronic Engineering*, vol. 187–188, pp. 66–77, Feb. 2018.
- [11] M. Khalilian and E. Adib, "Soft-single-switched dual forward-flyback PWM DC-DC converter with non-dissipative LC circuit," *2015 23rd Iranian Conference on Electrical Engineering*, May 2015.
- [12] A. Hassoune, M. Khafallah, A. Mesbahi, and T. Bouragba, "Smart topology of EVs in a PV-grid system based charging station," *2017 International Conference on Electrical and Information Technologies (ICEIT)*, Nov. 2017.
- [13] J. P. Torreglosa, P. García-Triviño, L. M. Fernández-Ramírez, and F. Jurado, "Decentralized energy management strategy based on predictive controllers for a medium voltage direct current photovoltaic electric vehicle charging station," *Energy Conversion and Management*, vol. 108, pp. 1–13, Jan. 2016.
- [14] C.-T. Tsai, T.-C. Liang, Y.-C. Kuo, and Y.-C. Luo, "An improved forward converter with PFC and ZVS features for split-phase charger applications," *Computers & Electrical Engineering*, vol. 51, pp. 291–303, Apr. 2016.
- [15] T.-C. Huang, Y.-G. Leu, Y.-C. Chang, S.-Y. Hou, and C.-C. Li, "An energy harvester using self-powered feed forward converter charging approach," *Energy*, vol. 55, pp. 769–777, Jun. 2013.
- [16] J. López, S. I. Seleme, P. F. Donoso, L. M. F. Morais, P. C. Cortizo, and M. A. Severo, "Digital control strategy for a buck converter operating as

a battery charger for stand-alone photovoltaic systems,” *Solar Energy*, vol. 140, pp. 171–187, Dec. 2016.

- [17] S. Venkatanarayanan and M. R. M. Nanthini, “Design and Implementation of SEPIC and Boost Converters for Wind and Fuel cell Applications,” *International Journal of Innovative Research in Science, Engineering and Technology*, vol. 3, no. 3, pp. 378–383, Mar. 2014,
- [18] J. C. Rosas-Caro, V. M. Sanchez, R. F. Vazquez-Bautista, L. J. Morales-Mendoza, J. C. Mayo-Maldonado, P. M. Garcia-Vite, and R. Barbosa, “A novel DC-DC multilevel SEPIC converter for PEMFC systems,” *International Journal of Hydrogen Energy*, vol. 41, no. 48, pp. 23401–23408, Dec. 2016.
- [19] K. Uddin, A. D. Moore, A. Barai, and J. Marco, “The effects of high frequency current ripple on electric vehicle battery performance,” *Applied Energy*, vol. 178, pp. 142–154, Sep. 2016.
- [20] Y. Guo, Z. Zhao, and L. Huang, “SoC Estimation of Lithium Battery Based on AEKF Algorithm,” *Energy Procedia*, vol. 105, pp. 4146–4152, May 2017.
- [21] D. A. Sbordone, B. Di Pietra, and E. Bocci, “Energy Analysis of a Real Grid Connected Lithium Battery Energy Storage System,” *Energy Procedia*, vol. 75, pp. 1881–1887, Aug. 2015.
- [22] G. Zubi, R. Dufo-López, M. Carvalho, and G. Pasaoglu, “The lithium-ion battery: State of the art and future perspectives,” *Renewable and Sustainable Energy Reviews*, vol. 89, pp. 292–308, Jun. 2018.
- [23] V. Lystianingrum, B. Hredzak, and V. G. Agelidis, “Multiple model estimator based detection of abnormal cell overheating in a Li-ion battery string with minimum number of temperature sensors,” *Journal of Power Sources*, vol. 273, pp. 1171–1181, Jan. 2015.
- [24] A. Hassoune, M. Khafallah, A. Mesbahi, and T. Bouragba “Power Management Strategies of Electric Vehicle Charging Station Based Grid Tied PV-Battery System,” *International Journal of Renewable Energy Research*, vol. 8, no. 2, pp. 851–860, Jun. 2018.
- [25] S. Guo, R. Xiong, K. Wang, and F. Sun, “A novel echelon internal heating strategy of cold batteries for all-climate electric vehicles application,” *Applied Energy*, vol. 219, pp. 256–263, Jun. 2018.
- [26] A. Hassoune, M. Khafallah, A. Mesbahi, L. Benaouinate, and T. Bouragba, “Control Strategies of a Smart Topology of EVs Charging Station Based Grid Tied RES-Battery,” *International Review of Electrical Engineering (IREE)*, vol. 13, no. 5, p. 385–396, Oct. 2018.



A. Hassoune was born in Settat, Morocco in 1993. He received the bachelor diploma in mathematical sciences in 2010, and the technical university degree in electrical engineering and computer science from the National High School of Technical Education, Mohammedia, Morocco, in 2012, and the master degrees from the Multidisciplinary Faculty of the Hassan I University, Khouribga, Morocco, in 2013, and the electrical engineer diploma in embedded systems and numerical control from the National School of Applied Sciences Khouribga, Morocco, 2015.

He joined the Hassan II University of Casablanca, ENSEM, Morocco, in 2015 as a PhD candidate at the Laboratory of Energy & Electrical Systems. His research interests include electric vehicles charging station with several publications in highly indexed journals.

Mr. Hassoune is a member of IEEE community with access to the world's largest technical professional organization dedicated to advancing technology for the benefit of humanity.



M. Khafallah is now a professor tutor in the Department Electrical Engineering at the Superior National School of Electricity and Mechanical (ENSEM), Hassan II University of Casablanca, Morocco. His main research interests the application of power electronics converts and motor drives.

He has published a lot of research papers in international journals, conference proceedings as well as chapters of books.



A. Mesbahi received the M.A degree from ENSET, Rabat, Morocco in 1990 and the DEA diploma in information processing in 1997 from Hassan II University, Faculty of sciences Ben M'sik Casablanca, Morocco. He obtained the Ph.D. degree in engineering sciences from ENSEM Casablanca, Morocco in 2013.

Until 2013, he was a teacher in electrical engineering department at ENSET Mohammedia Morocco. Actually, he acts as assistant professor in electrical engineering department at ENSEM, Casablanca, Morocco. His research in Energy and Electrical Systems Laboratory (LESE), is focused on sensorless control and advanced command applied to electrical machines and control of renewable energy systems. He is also an associated research member of SSDIA Laboratory based in ENSET, Mohammedia, Morocco.



T. Bouragba is the Associate Professor, Department of Physics in EIGSICA engineering school of industrial system, Casablanca, Morocco. He completed his M.Sc, Ph.D degrees in Physics from Blaise Pascal University, Clermont-Ferrand, France. He worked as Replication Process Manager for 3 years at Nemotek Technologies SA, Rabat, Morocco. He had participated in many national and international workshop, seminars and conferences. He has 3 years of experience in material research and 3 years in teaching. His area of research includes material science, nanotechnology for cells application. His ongoing activities are focusing on renewable energies.